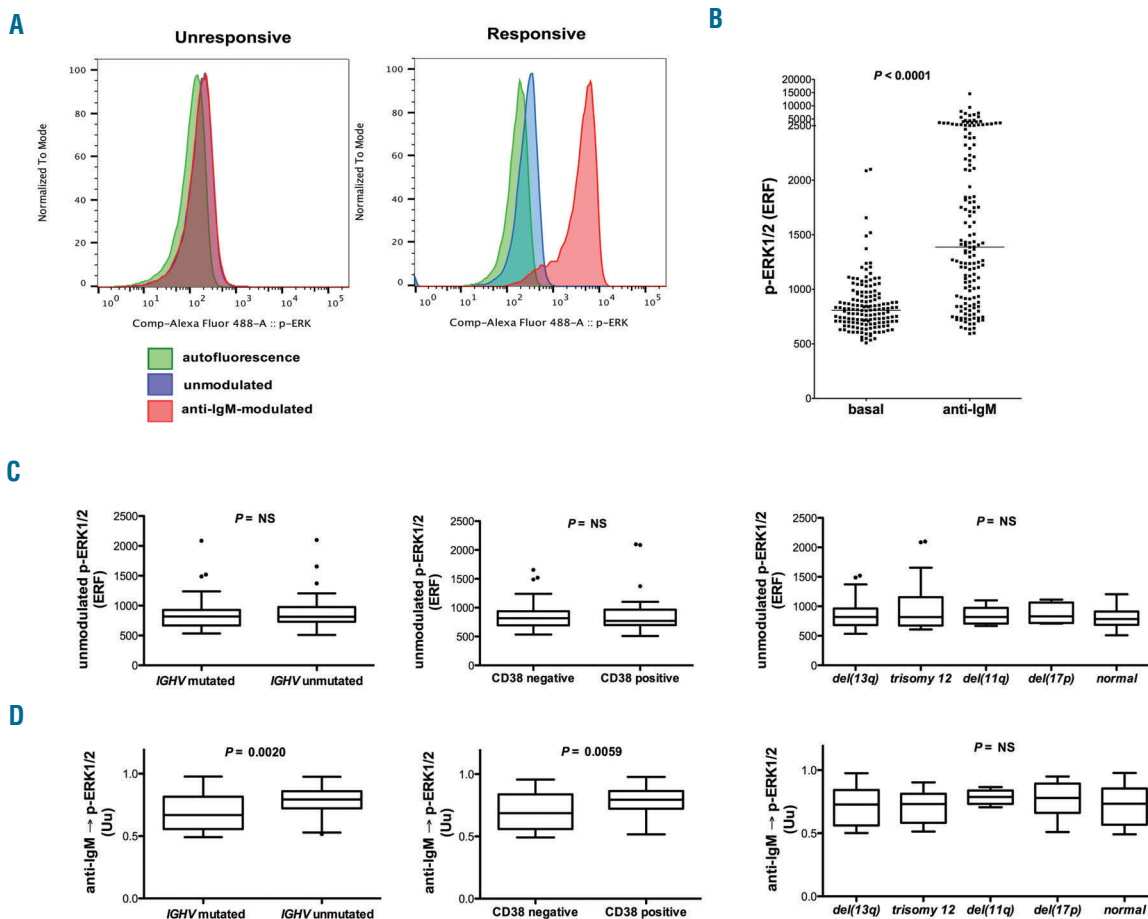


## Integration of B-cell receptor-induced ERK1/2 phosphorylation and mutations of *SF3B1* gene refines prognosis in treatment-naïve chronic lymphocytic leukemia

Signaling events downstream of the B-cell receptor (BCR) are key determinants of the clinical behavior of chronic lymphocytic leukemia (CLL).<sup>1,2</sup> Extracellular signal-regulated kinase 1/2 (ERK1/2) is a major pathway downstream of BCR stimulation.<sup>3,4</sup> In a recent study, applying a single cell network profiling (SCNP) assay<sup>5</sup> to independent sets of CLL samples, we characterized functional elements of the BCR signaling network associated with clinical outcomes in CLL and validated BCR-induced ERK1/2 phosphorylation as a significant, independent predictor of faster clinical progression in CLL.<sup>6</sup> Novel recurrent mutated genes have recently been associated with progressive or high-risk disease and a dismal outcome in CLL.<sup>7,8</sup> Gene alterations occur during cancerous transformation and evolution of the malignant clone, most likely favored by

signals from the BCR and microenvironment. Despite the established driving role of BCR signaling and gene mutations in CLL, little is known about the association between functional BCR responses and specific genetic alterations. Investigating the physiology of BCR signaling in the genetic context would add useful information to improve prognostic classification of CLL patients and gain deeper insights into pathobiological mechanisms. Herein, we investigated the impact of integrated BCR-induced ERK1/2 phosphorylation and recurrent gene mutations on prognosis of untreated CLL. We found that integrated dynamic ERK1/2 phosphorylation and *SF3B1* mutations are associated with the risk of disease progression and enable identification of a novel intermediate-risk group of patients.

ERK1/2 phosphorylation (pERK1/2) was measured by SCNP<sup>5,6</sup> in 152 treatment-naïve CLL cell samples (*Online Supplementary Table S1*), in basal condition and following BCR stimulation with anti-IgM (Figure 1A,B). In the basal condition, we detected no differences in pERK1/2 between subgroups of patients defined by *IGHV* mutational status (UM: unmutated; M: mutated), CD38 expres-



**Figure 1. ERK1/2 phosphorylation in B cells from CLL patients.** (A) Representative flow cytometry histograms of pERK1/2 in the basal condition or following BCR modulation with anti-IgM in CD5<sup>+</sup>/CD19<sup>+</sup> cells from CLL patients, compared with autofluorescence signals. (B) pERK1/2 in CLL patients, in the basal condition and following anti-IgM modulation (n=152). Data are expressed as equivalent number of reference fluorophores (ERF). The results for basal and anti-IgM-modulated CLL cells were compared by the two-sample Wilcoxon signed rank sum test. The lines indicate the medians. The Y-axis is expanded on low values. (C-D) SCNP signals of pERK1/2 in the basal condition (C) and in response to anti-IgM stimulation (D) was associated with *IGHV* status (n=134), CD38 expression (n=152), and cytogenetic mutations (n=141). Different sample sizes depend on availability of biological parameters. Data are expressed as equivalent number of reference fluorophores (ERF) (C) and Uu (D) and represented as Tukey boxes and whiskers. The Mann-Whitney test and Kruskal-Wallis test were used for comparisons. NS: not significant.

sion and cytogenetic alterations (Figure 1C). In contrast, pERK1/2 in response to BCR stimulation (anti-IgM→pERK1/2) was higher in UM-CLL than in M-CLL and higher in CD38-positive cases than in CD38-negative cases (Figure 1D). Moreover, higher anti-IgM→pERK1/2 was associated with treatment requirement during follow-up (Online Supplementary Table S2).

Mutations of *NOTCH1*, *SF3B1*, *TP53*, *BIRC3*, and *MYD88* genes were examined in CLL samples for which DNA was available (146/152) by polymerase chain reaction amplification and Sanger sequencing (details in Online Supplementary Data). Due to the low number of *BIRC3* (n=2/146) and *MYD88* (n=2/146) mutations, these genes were excluded from analysis.

*NOTCH1* mutations were detected in 17/146 (12%) samples. Of these 17 patients, 15 (88%) carried missense mutations whereas 2/17 (12%) had non-sense events: these latter were excluded from the analysis. *NOTCH1* mutations were associated with higher CD38 expression and showed a trend toward association with trisomy 12 (Figure 2A; Online Supplementary Table S3). No associations were found between *NOTCH1* mutations and anti-IgM→pERK1/2 (Figure 2A; Online Supplementary Table S3).

*SF3B1* genetic lesions were detected in 19/146 (13%) patients. These mutations were associated with UM-*IGHV* status (Figure 2A; Online Supplementary Table S3) and more frequently detected in advanced (Binet stage B-C) stage disease and in patients requiring treatment during follow-up (Online Supplementary Table S2). Of note, cases harboring *SF3B1* mutations also exhibited a higher anti-IgM→pERK1/2 (Figure 2A-B; Online Supplementary Table S3). Given the strong association between anti-IgM→pERK1/2 and UM-*IGHV* status (Figures 1D and 2A), we sought to assess the influence of *IGHV* status on the association between anti-IgM→pERK1/2 and *SF3B1* mutations. Superimposition of *IGHV* status revealed that in M-CLL *SF3B1* mutations did not identify CLL subgroups with different anti-IgM→pERK1/2 (Figure 2B). Therefore, in M-CLL *SF3B1* mutations apparently did not have a significant impact on anti-IgM→pERK1/2. In UM-

CLL, *SF3B1*-mutated cases exhibited a higher anti-IgM→pERK1/2 than wild-type (wt) *SF3B1* cases (Figure 2B). The more frequent association of UM-*IGHV* with ERK1/2 responsiveness to BCR is, therefore, mainly explained by UM-CLL samples that harbor *SF3B1* mutations.

*TP53* gene mutations were detected in 11/146 (8%) cell samples, with one patient harboring two mutations. As expected, *TP53* lesions were enriched in patients with del(17p) (Figure 2A; Online Supplementary Table S3). While cases with *TP53* lesions exhibited a trend toward association with high anti-IgM→pERK1/2, cases with p53 dysfunction [*TP53* lesions and/or del(17p)] showed no association with high anti-IgM→pERK1/2 (Figure 2A; Online Supplementary Table S3).

Concurrent mutations were detected in only two cases (coexisting *NOTCH1* and *TP53* mutations) and their association with pERK1/2 was not, therefore, investigated.

To assess the impact of pERK1/2 integrated with gene mutations on disease progression, measured as time to first treatment (TTFT), we examined time-to-event modeling utilizing ERK1/2 SCNP data, recurrent gene mutations, *IGHV* status, CD38 expression, and cytogenetic alterations – alone and in combination – in the whole set of patients for whom all studied biological and TTFT data were available (n=125/152). Univariate time-to-event analysis identified higher anti-IgM→pERK1/2 (Figure 3A), mutated *SF3B1* (Figure 3B), UM-*IGHV* ( $P<0.0001$ ), and CD38-positivity ( $P=0.001$ ) as significant, independent predictors of shorter TTFT. While high anti-IgM→pERK1/2 was not associated with shorter TTFT in the comprehensive multivariate analysis, in a bivariate time-to-event analysis high anti-IgM→pERK1/2 and *SF3B1* mutation were found to be independent, significant parameters of prognosis (Online Supplementary Table S4A). Remarkably, integrating anti-IgM→pERK1/2 data and *SF3B1* mutation, three independent prognostic categories were identified: a low-risk group (n=42; patients requiring treatment=26%; median TTFT=40 months) comprised patients with low anti-IgM→pERK1/2 and wt *SF3B1*; an intermediate-risk

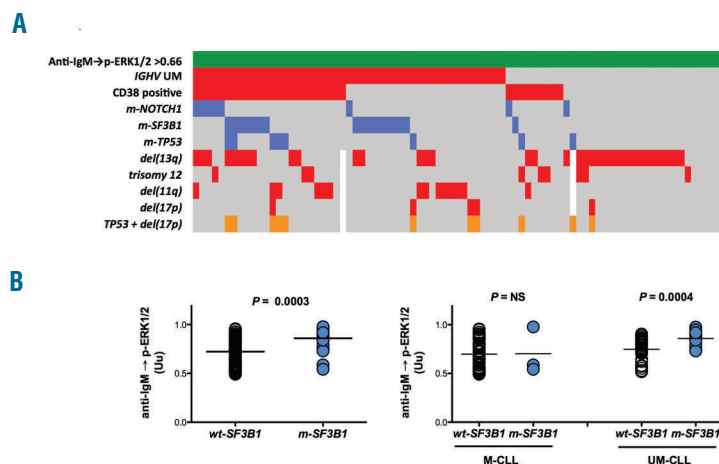


**Figure 2. Association of ERK1/2 phosphorylation in response to BCR stimulation with gene mutations.** (A) ERK1/2 phosphorylation in response to anti-IgM stimulation (anti-IgM→pERK1/2) (n=152), expressed by the Uu metric, was associated with *IGHV* status, CD38 expression, *NOTCH1*, *SF3B1* and *TP53* mutations, and cytogenetic mutations. Rows correspond to parameters and columns represent individual patients. Data are colored in: green = high IgM→pERK1/2, red = positive for standard prognostic parameters, blue = presence of gene mutation, orange = positive for p53 dysfunction (*TP53* mutation and/or del(17p)), gray = negative, white = no available data. (B) anti-IgM→pERK1/2, expressed as Uu values, was associated with *SF3B1* mutation in the entire set of patients (left panel; n=146) and in the UM-CLL subset (right panel). Lines represent the mean values. Comparisons were performed using the Mann-Whitney test (left panel) and Kruskal-Wallis test (right panel).

group (n=66; patients requiring treatment=48%; median TTFT=34 months) included patients with low anti-IgM→pERK1/2 and mutated *SF3B1* or high anti-IgM→pERK1/2 and wt *SF3B1*; and a high-risk group (n=17; patients requiring treatment=82%, median TTFT=3 months) comprised patients with high anti-IgM→pERK1/2 and mutated *SF3B1* (Figure 3C).

A subset of Binet stage A patients for whom all biological and TTFT data were available (n=90/112) was then analyzed. Univariate time-to-event analysis identified increased anti-IgM→pERK1/2 (Figure 3D), mutated *SF3B1* (Figure 3E), mutated *TP53* ( $P=0.001$ ), *UM-IGHV* ( $P<0.0001$ ), and CD38-positivity ( $P=0.0006$ ) as significant, independent predictors of shorter TTFT. The bivariate time-to-event analysis identified high anti-IgM→pERK1/2 and *SF3B1* mutation as independent significant variables in terms of TTFT (Supplementary Table S4B). Integrating anti-IgM→pERK1/2 and *SF3B1* mutation, we could stratify early-stage patients into three independent prognostic categories: a low-risk group (n=33; patients requiring treatment=18%, median TTFT=47 months) comprised patients with low anti-IgM→pERK1/2 and wt *SF3B1*; an intermediate-risk group (n=49; patients requiring treatment=37%, median TTFT=42 months) included patients with low anti-IgM→pERK1/2 and mutated *SF3B1* or high anti-

IgM→p-ERK1/2 and wt *SF3B1*; and a high-risk group (n=8; patients requiring treatment =75%, median TTFT=16 months) comprised patients with high anti-IgM→pERK1/2 and mutated *SF3B1* (Figure 3F).

In this study, we measured ERK1/2 response to BCR in association with *NOTCH1*, *SF3B1*, *TP53* mutations with the aim of integrating, for the first time, dynamic properties of BCR activation and driver-gene mutations in a prognostic model for treatment-naïve CLL. Our data reveal that integrating dynamic ERK1/2 phosphorylation and *SF3B1* mutational status improves the prognostic potential of pERK1/2 and *SF3B1* alone and identifies three groups of patients with distinct risks of disease progression.

The finding that high anti-IgM→pERK1/2 identifies a subgroup of CLL treatment-naïve patients with a more aggressive disease and a faster clinical progression confirms our previous data obtained from patients with early-stage disease<sup>6</sup> and extend them to patients with advanced-stage disease. Overall, these data identify ERK1/2 as a relevant node on the route of BCR signaling, which is able to capture the behavior of other components of the pathway. In line with this, ERK1/2 functions as a survival pathway<sup>9</sup> and is required for cell cycle progression in CLL.<sup>10</sup> Of note, a recent study showed that novel CLL driver mutations affect the ERK pathway, with 8.7% of patients carrying at

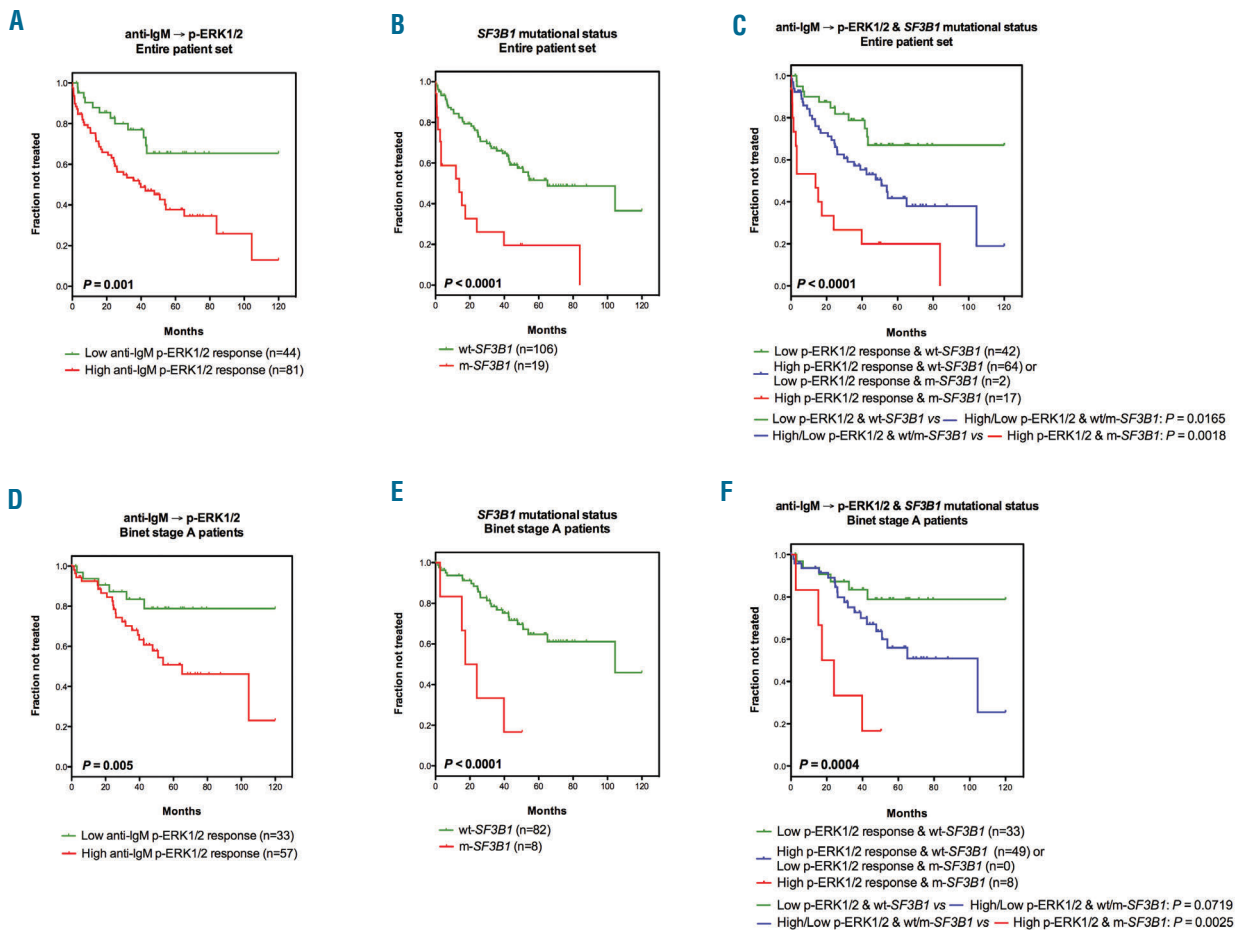


**Figure 3. Kaplan-Meier curves of time to first treatment (TTFT).** Kaplan-Meier curves of TTFT for the entire patient set for which biological parameters and clinical data were available (n=125/152, A-C) or for the Binet stage A patients for whom biological parameters and clinical data were available (n=90/112, D-F). Curves were defined by pERK1/2 response to BCR (anti-IgM→pERK1/2), using the pre-specified 0.66 Uu cut-off (A,D), the presence of *SF3B1* mutations (B,E), or the integrated anti-IgM→pERK1/2 data (cut-off=0.66) and *SF3B1* mutations (C,F).

least one gene mutation in this pathway.<sup>11</sup> Interestingly, the response of ERK1/2 to BCR, rather than its basal phosphorylation state, is associated with standard prognostic parameters (UM-IGHV and CD38 positivity, but not cytogenetic alterations) and disease progression, supporting the determinant role of dynamic properties of BCR signaling in CLL. These data are in agreement with a recent study by D'Avola *et al.* showing that BCR responsiveness, measured as percentage of intracellular Ca<sup>2+</sup> mobilization, is associated with UM-IGHV and CLL aggressiveness.<sup>2</sup> In contrast with our results, that study showed an association between BCR responsiveness and trisomy 12 and del(17p). These discrepancies might be due to differences in sets of patients and measurements of BCR response.

To measure ERK1/2 signaling in this study, we used SCNP, a phospho-specific assay based on flow cytometry, which provided ERK1/2 readout metrics for developing a mathematical model for the prediction of CLL progression.<sup>5,6</sup> Overall, this study confirms that SCNP can capture biologically and clinically relevant information on pathological cells.

As expected, mutations of *NOTCH1*, *SF3B1* and *TP53* genes were more frequently detected in patients with unfavorable clinico-biological features.<sup>8,12,13</sup> This was specifically pronounced for *SF3B1*, whose mutations were enriched in UM-CLL, advanced disease, and patients requiring treatment during follow-up. *SF3B1* mutations were also associated with a higher response of ERK1/2 to BCR, specifically in UM-CLL. In contrast, D'Avola *et al.* revealed differential BCR responses between wt and mutated *SF3B1* in M-CLL but not in UM-CLL.<sup>2</sup> Besides differences in the BCR-response measurements, this discrepancy may be due to the low number of cases with *SF3B1* mutations (7 in the study by D'Avola *et al.* and 3 in ours). Further studies with larger series of patients are required to address this issue.

Only *SF3B1* mutations integrated with anti-IgM→pERK1/2 can refine prognosis in CLL, which might suggest a direct effect of *SF3B1* mutations on BCR signaling. *SF3B1* is a core component of the RNA splicing machinery<sup>14</sup> and, among other effects, *SF3B1* mutations might induce alternative splicing of the BCR component CD79b. A change in the balance between the entire CD79b transcript and the alternative spliced form could account for altered BCR expression and function in CLL.<sup>15</sup>

In conclusion, this study shows that integrated ERK1/2 response to BCR stimulation and *SF3B1* gene mutations refine prognosis in CLL and may form the basis for future investigations aimed at validating an integrated prognostic model including dynamic properties of BCR and *SF3B1* mutation in CLL.

Chiara Cavallini,<sup>1</sup> Carlo Visco,<sup>2</sup> Santosh Putta,<sup>3</sup> Davide Rossi,<sup>4</sup> Elda Mimiola,<sup>5</sup> Norman Purvis,<sup>6</sup> Ornella Lovato,<sup>1</sup> Omar Perbellini,<sup>2</sup> Erika Falisi,<sup>2</sup> Monica Facco,<sup>7</sup> Livio Trentin,<sup>7</sup> Maria G. Romanelli,<sup>8</sup> Gianpietro Semenzato,<sup>7</sup> Achille Ambrosetti,<sup>5</sup> Gianluca Gaidano,<sup>9</sup> Giovanni Pizzolo,<sup>5</sup> Alessandra Cesano<sup>10</sup> and Maria T. Scupoli<sup>1,5</sup>

<sup>1</sup>Research Center LURM, University of Verona, Italy; <sup>2</sup>Department of Cell Therapy and Hematology, San Bortolo Hospital, Vicenza, Italy; <sup>3</sup>Qognit Inc., Foster City, CA, USA; <sup>4</sup>Hematology, Oncology Institute of Southern Switzerland and Institute of Oncology Research, Bellinzona, Switzerland; <sup>5</sup>Department of Medicine, Section of Hematology, University of Verona, Italy; <sup>6</sup>Pierian Biosciences, Franklin, TN, USA; <sup>7</sup>Department of Medicine, Hematology and Clinical

Immunology Branch, University of Padua, Italy; <sup>8</sup>Department of Neurosciences, Biomedicine and Movement Sciences, Section of Biology and Genetics, University of Verona, Italy; <sup>9</sup>Department of Translational Medicine, Division of Hematology, Amedeo Avogadro University of Eastern Piedmont, Novara, Italy and <sup>10</sup>NanoString, Inc, Seattle, WA, USA

*Acknowledgments:* the authors would like to thank all patients who donated samples for this study. Grant support for this study was provided by Fondazione Cassa di Risparmio di Verona, Vicenza, Belluno e Ancona and Associazione Italiana Ricerca sul Cancro (AIRC), Milan, Italy (grant #6599) (MGR, GS, GP, and MTS); Fondazione Cassa di Risparmio di Verona, Vicenza, Belluno e Ancona (grant #2015.0872) (MTS); Special Program Molecular Clinical Oncology 5x1000 No. 10007 (GG); AIRC, Milan, Italy (GG); and Progetto Ricerca Finalizzata RF-2011-02349712, Ministero della Salute, Rome, Italy (GG).

Correspondence: mariateresa.scupoli@univr.it  
doi:10.3324/haematol.2016.154450

Information on authorship, contributions, and financial & other disclosures was provided by the authors and is available with the online version of this article at [www.haematologica.org](http://www.haematologica.org).

## References

- Packham G, Krysov S, Allen A, et al. The outcome of B-cell receptor signaling in chronic lymphocytic leukemia: proliferation or anergy. *Haematologica*. 2014;99(7):1138–1148.
- D'Avola A, Drennan S, Tracy I, et al. Surface IgM expression and function are associated with clinical behavior, genetic abnormalities, and DNA methylation in CLL. *Blood*. 2016;128(6):816–826.
- Gauld SB, Dal Porto JM, Cambier JC. B cell antigen receptor signaling: roles in cell development and disease. *Science*. 2002;296(5573):1641–1642.
- Scupoli MT, Pizzolo G. Signaling pathways activated by the B-cell receptor in chronic lymphocytic leukemia. *Expert Rev Hematol*. 2012;5(3):341–348.
- Irish JM, Hovland R, Krutzik PO, et al. Single cell profiling of potentiated phospho-protein networks in cancer cells. *Cell*. 2004; 118(2):217–228.
- Cesano A, Perbellini O, Evensen E, et al. Association between B-cell receptor responsiveness and disease progression in B-cell chronic lymphocytic leukemia: results from single cell network profiling studies. *Haematologica*. 2013;98(4):626–634.
- Puente XS, Beà S, Valdés-Mas R, et al. Non-coding recurrent mutations in chronic lymphocytic leukaemia. *Nature*. 2015; 526(7574):519–524.
- Fabbri G, Dalla-Favera R. The molecular pathogenesis of chronic lymphocytic leukaemia. *Nat Rev Cancer*. 2016;16(3):145–162.
- Paterson A, Mockridge CI, Adams JE, et al. Mechanisms and clinical significance of BIM phosphorylation in chronic lymphocytic leukemia. *Blood*. 2012;119(7):1726–1736.
- Krysov S, Dias S, Paterson A, et al. Surface IgM stimulation induces MEK1/2-dependent MYC expression in chronic lymphocytic leukemia cells. *Blood*. 2012;119(1):170–179.
- Landau DA, Tausch E, Taylor-Weiner AN, et al. Mutations driving CLL and their evolution in progression and relapse. *Nature*. 2015;526(7574):525–530.
- Wang L, Lawrence MS, Wan Y, et al. SF3B1 and other novel cancer genes in chronic lymphocytic leukemia. *N Engl J Med*. 2011;365(26):2497–2506.
- Rossi D, Gaidano G. The clinical implications of gene mutations in chronic lymphocytic leukaemia. *Br J Cancer*. 2016;114(8):849–854.
- Hahn CN, Scott HS. Spliceosome mutations in hematopoietic malignancies. *Nat Genet*. 2011;44(1):9–10.
- Alfarano A, Indraccolo S, Circo P, et al. An alternatively spliced form of CD79b gene may account for altered B-cell receptor expression in B-chronic lymphocytic leukemia. *Blood*. 1999;93(7):2327–2335.